The Astrophysical Journal, 610:673–678, 2004 August 1

POSSIBILITY OF MAGNETIC MASS DETECTION BY THE NEXT GENERATION OF MICROLENSING EXPERIMENTS

Sohrab Rahvar[1,2] and Farhang Habibi[3]
Received 2003 November 10; accepted 2004 April 6

ABSTRACT

We study the possibility of magnetic mass detection using the gravitational microlensing technique. Recently, the theoretical effect of magnetic mass in NUT space on the microlensing light curve has been studied. It has been shown that in the low photometric signal-to-noise ratio and sampling rate of MACHO experiment light curves, no signature of the NUT factor has been found. In order to increase the sensitivity of magnetic mass detection, we propose a systematic search for microlensing events, using the currently running alert systems and complementary telescopes for monitoring Large Magellanic Clouds stars. This observation strategy provides the lowest observable limit of the NUT factor, and we calculate the magnetic mass detection efficiency. This survey method for gravitational microlensing detection can also be used as a tool for searching other exotic spacetimes.

Subject headings: cosmology: observations — cosmology: theory — dark matter — gravitational lensing — relativity

1. INTRODUCTION

A gravitational microlensing method for detecting massive compact halo objects (MACHOs) in the Milky Way halo has been proposed by Paczyński (1986). Many groups have contributed to this experiment and have detected hundreds of microlensing candidates in the direction of the Galactic bulge, spiral arms, and Large and Small Magellanic Clouds (LMC and SMC). Because of the low probability of microlensing detection, less than 20 events have been observed by the EROS and MACHO groups in the direction of the Magellanic clouds (Lasserre et al. 2000; Alcock et al. 2000). Not only do the low statistics cause ambiguities in identifying the galactic model of the Milky Way, but also in some cases the microlensing results are at variance with the results of other observations (Gates & Gyuk 2001).

Comparing LMC microlensing events with theoretical galactic models can give us the mean mass of MACHOs and the fraction of halo mass in the form of MACHOs. If we use a Dirac delta mass function for the MACHOs, the mass of MACHOs in a standard halo model is about $\sim 0.5\ M_{\odot}$. This means that the initial mass function of MACHO progenitors in the Galactic halo should be different from that of the disk, because we see neither the low-mass stars that should still exist nor heavier stars that would have exploded in the form of supernova (Adams & Laughlin 1996; Chabrier et al. 1996). Another contradiction is that if there were as many white dwarfs in the halo as suggested by the microlensing experiments, they would increase the abundance of heavy metals via Type I supernova explosions (Canal et al. 1997). Recently, Green & Jedamzik (2002) and Rahvar (2004) also showed that the observed distribution of the duration of microlensing events is significantly narrower than what is expected from standard and nonstandard galactic halo models.

The problems mentioned here could be a good motive for the next generation of microlensing experiments. The new surveys will have the potential to increase the number of microlensing candidates and reduce the ambiguities due to Poisson statistics. Other improvements to the new surveys could include higher sampling rates and higher precision photometry of the light curves. More precise light curves will enable us to distinguish deviations between the standard and nonstandard light curves due to parallax or source finite-size effects (Rahvar et al. 2003). In so-called nonstandard microlensing candidates, the degeneracy can be partially broken between lens parameters, such as the distance and the mass of a lens. A better determination of the distance and the mass distributions of the lenses can help us to better identify the Milky Way halo model (Evans 1994).

Although the effects mentioned here exist in Schwarzschild space, it is also possible that a lensing MACHO resides in an exotic spacetime such as Kerr or NUT space (Newman et al. 1963). Deviation of the spacetime from the Schwarzschild metric would cause deviation of the microlensing light curve from the standard one. Thus, studying the microlensing light curves can be used not only to determine the dark matter in the form of MACHOs, but also as a unique tool to explore other exotic spacetimes as well.

Nouri-Zonoz & Lynden-Bell (1997) considered the gravitational lensing effect on light rays passing by a NUT hole, using the fact that all the geodesics in the NUT space, including the null ones, lie on cones. Rahvar & Nouri-Zonoz (2003) have extended this work to the microlensing light curve in NUT space and tested the possible existence of magnetic mass on the light curves of the MACHO group microlensing candidates. According to the analysis of the light curves, no magnetic mass effect has been found. Although the results showed that the effect of the NUT factor is almost negligible, one cannot rule out the existence of NUT charge on that basis. The next generation of microlensing experiments may prove the existence (or nonexistence) of magnetic mass through a more careful study of microlensing light curves.

In this work we simulate the microlensing light curves in the NUT metric according to a strategy for the next generation of microlensing surveys. The aim of this work is to obtain the

[1] Department of Physics, Sharif University of Technology, P.O. Box 11365–9161, Tehran, Iran; rahvar@sharif.edu.
[2] Institute for Studies in Theoretical Physics and Mathematics, P.O. Box 19395–5531, Tehran, Iran.
[3] Department of Physics, Iran University of Science and Technology, Narmak, Tehran 16844, Iran.

observational efficiency for the magnetic mass detection and to find the lowest observable limit for the NUT charge. Large Magellanic Cloud (LMC) stars are chosen as the target stars for monitoring. The advantage of using LMC stars as compared to spiral arm and the Galactic bulge stars is the lower contamination by blending and source finite-size effects, which can affect the NUT light curves. The other advantage of LMC monitoring is that it enables us to increase the microlensing statistics to put a better limit on the mass of the lenses and the mass fraction of the galactic halo in form of MACHOs.

The organization of the paper is as follows. In § 2, we give a brief account on the microlensing light curve in the NUT metric and compare it with the Schwarzschild case. In § 3, we introduce the observational strategy and perform a Monte Carlo simulation to generate the microlensing light curves. Section 4 contains the fitting process used for the simulated light curves to obtain the observational efficiency of the magnetic mass detection. The results are discussed in § 5.

2. GRAVITATIONAL MICROLENSING IN SCHWARZSCHILD AND NUT METRICS

The gravitational lensing effect occurs when the impact parameter of a lens with respect to the undeflected observer-source line of sight is small enough that the deviation of the source shape becomes detectable. In the case of a pointlike source, the deflection angle is too small to be resolved by current telescopes. This type of gravitational lensing, which amplifies the brightness of the background star, is called gravitational microlensing. In the Schwarzschild metric the magnification is given by (Paczyński 1986)

$$A(t) = \frac{u(t)^2 + 2}{u(t)\sqrt{u(t)^2 + 4}}, \tag{1}$$

where $u(t) = \left\{u_0^2 + [(t - t_0)/t_{\rm E}]^2\right\}^{1/2}$ is the impact parameter (position of the source in the deflector plane normalized by the Einstein radius, $R_{\rm E}$), and $t_{\rm E}$ is the Einstein crossing time (duration of event), defined by $t_{\rm E} = R_{\rm E}/v_t$, where v_t is the transverse velocity of the deflector with respect to the line of sight. The Einstein radius is given by $R_{\rm E}^2 = 4GMD/c^2$, where M is the mass of the deflector and $D = D_l D_{ls}/D_s$, where D_l, D_{ls}, and D_s are the observer-lens, lens-source, and observer-source distances, respectively. The only physical parameter that can be obtained from a light curve is the duration of the event, which is a function of the lens parameters such as mass, distance of lens from the observer, and relative transverse velocity of the lens with respect to our line of sight.

In the case of gravitational microlensing, the configuration of the lens changes within a timescale of dozen of days, while on cosmological scales the lensing configuration is almost static. Since the magnification factor depends on the spacetime metric, the gravitational microlensing technique may also be a useful tool for exploring other exotic metrics such as NUT space. In NUT space the magnification due to microlensing depends on extra factor (magnetic mass) compared to Schwarzschild space. It should be mentioned that NUT space reduces to Schwarzschild space when the magnetic mass (l) is zero.[4] Thus, we expect that the microlensing amplification reduces to equation (1) for zero magnetic mass. Rahvar & Nouri-Zonoz (2003) obtained the magnification in this spacetime as

$$A(u) = \frac{2 + u^2}{u\sqrt{4 + u^2}} + \frac{8R^4(2 + u^2)}{u^3(4 + u^2)^{3/2}} + \mathcal{O}(R^8) + \ldots, \tag{2}$$

where $R_{\rm NUT} = (2lD)^{1/2}$ is defined as the NUT radius (analogous to the Einstein radius), and l is the magnetic mass of the lens. The parameter R in equation (2) is defined by dividing the NUT radius by the Einstein radius, $R = R_{\rm NUT}/R_{\rm E}$. It can be seen that in NUT space the magnification factor, as in the Schwarzschild case, is symmetric with respect to time. The extra second term implies a larger relative maximum of the magnification factor for a given minimum impact parameter. We also find a shape deviation of the light curve with respect to the case of Schwarzschild metric.

The detectability of the NUT factor through studying microlensing depends on the light-curve quality (i.e., sampling rate and photometric error bars). In the next section we introduce a new strategy for microlensing observations in order to improve the microlensing light curves, from the point view of both the sampling rate and the photometric precision.

3. LIGHT CURVE SIMULATION IN NUT SPACE

The observation strategy is based on using a survey as an alert system for microlensing detection, with a follow-up setup. EROS is one of the groups that used an alert system to trigger observation of ongoing microlensing events. We simulate EROS-like telescope with the same sampling rate, considering 70% clear sky at La Silla during the observable seasons of the LMC. A follow-up telescope is considered to observe, with 1% photometry precision and sampling rate of at least once per night, those events that have been triggered by the first telescope. Here our aim is to simulate microlensing light curves in NUT space by using the observational strategy mentioned above.

It should be noted that there are at least two other important effects, blending and source finite-size effects, that can change the light curves in a symmetric manner that mimics the NUT factor. Those effects are important because they may dominant over the effect of the NUT factor in the light curves. Thus, before starting the simulation procedure we give a brief account of those effects, and we include them in generating microlensing light curves in NUT space.

The blending effect is due to the mixing of the light of a lensed star and its neighbors, which is given as

$$F(t) = F_b + A(t)F_s, \tag{3}$$

where $F(t)$ is the measured flux, F_s is the flux of the lensed source, F_b is from the vicinity of lensed source, and $A(t)$ is the amplification (Wozniak & Paczynski 1997). This effect is described by the blending parameter, which is defined as $b = F_s/(F_s + F_b)$; the observed magnification factor can be written as

$$A_{\rm obs}(t) = 1 + b[A(t) - 1]. \tag{4}$$

The second altering effect on a light curve in NUT space is the source finite-size effect, which is caused by the nonzero size of projected source star on the lens plane. In this case, different parts of the source star are amplified by different factors. The relevant parameter of this effect is the projected size of the

[4] NUT space is give by the metric $ds^2 = f(r)(dt - 2l\cos\theta d\phi)^2 - [1/f(r)]dr^2 - (r^2 + l^2)(d\theta^2 + \sin^2\theta d\phi^2)$, where $f(r) = 1 - 2(Mr + l^2)/(r^2 + l^2)$.

source radius on the lens plane, normalized to the corresponding Einstein radius ($U = xR/R_E$), where $x = D_l/D_s$ is the ratio of lens and source distances from the observer, and R is the size of the source radius. In the case of close source-lens distance compared to the observer-source distance, this effect becomes important.

To find the best field of source stars, we compare possible fields of observation, such as the Galactic bulge, the spiral arms, and the Magellanic clouds to find the least blending and source finite-size effects. In the direction of the Galactic bulge, the blending effect is high, since the field of target stars is crowded, except for the clump giants (Popowski et al. 2000). For the spiral arm stars, the blending effect is less than toward the Galactic bulge, while the source finite-size effect due to self-lensing by the spiral arm stars is considerable. For the SMC, according to the blending and parallax studies of long-duration events (Palanque-Delabrouille et al. 1998), it seems that SMC is quite elongated along our line of sight, with a depth varying from a few kpc (the tidal radius of the SMC is of the order of 4 kpc) to as much as 20 kpc. Thus, because of high blending and source finite-size effects, the SMC is not suitable for searching gravito-magnetic parameters. It seems that the LMC is the best choice for this study. The other advantage of using this field is increasing the microlensing statistics, which can be used in dark matter studies of the Galactic halo.

In our simulation, we use the distribution of the blending factor according to the reconstructed blending parameter that has been obtained by the best fit to the LMC microlensing events. For the source finite-size effects of LMC stars, which become important in the case of self-lensing, we first compare relative self-lensing abundance to Galactic halo lensing and then evaluate the finite-size effect of those events on the light curves.

Comparing the optical depth for the standard Galactic halo model, $\tau_{\rm halo} = 1.2^{+0.4}_{-0.3} \times 10^{-7}$ (Alcock et al. 2000), with the optical depth obtained from the LMC itself, $\tau_{\rm self\text{-}lens} = [0.47\text{–}7.84] \times 10^{-8}$ (Gyuk et al. 2000), mean value 2.4×10^{-8}, shows that the expected number of microlensing events caused by halo MACHOs is about 1 order of magnitude more than that of the LMC. The optical depth value of LMC self-lensing can be confirmed by studying the parallax effect on the light curves. Rahvar et al. (2003) showed that using the same observational strategy proposed here, if the self-lensing is dominant, very few lenses (only those that belong to the disk) produce a detectable parallax effect.

In order to evaluate the source finite-size effect on the microlensing light curves of the LMC, we perform a Monte Carlo simulation to produce the distribution of the relevant parameter U. We use the LMC model introduced by Gyuk et al. (2000) to see the matter distribution in our line of sight. The probability of a microlensing event by a LMC lens at a given distance from us is

$$\frac{d\Gamma(x)}{dx} \propto \sqrt{x(1-x)}\rho(x),$$

where $\rho(x)$ is the matter density distribution of LMC.

The source stars in the LMC are chosen according to their color-magnitude distribution. We use the mass-radius relation (Demircan & Kahraman 1990) to evaluate the radii of stars in our simulation. The radii of source stars are projected on the lens plane and normalized to the corresponding Einstein radius to obtain the distribution of U for the LMC self-lensing events. The mean value of U according to our simulation is about 10^{-3}, which we applied to obtain the gravitational microlensing light curves. For an impact parameter as small as $u_0 = 0.01$, where the NUT factor becomes important, the maximum magnification difference of a standard light curve and that obtained by considering source finite-size effect is about 1%. On the one hand, this difference is less than our photometric accuracy; on the other hand, the optical depth from self-lensing is 1 order of magnitude smaller than that of the galactic halo. The conclusion is that the source finite-size effect is not important in our analysis.

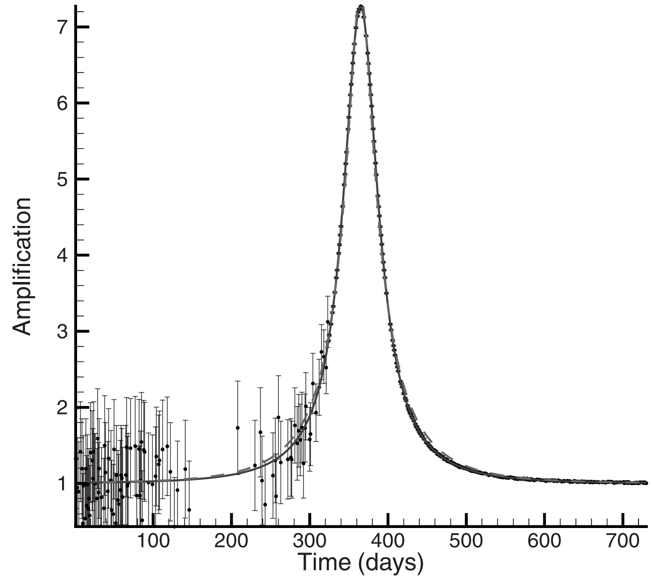

FIG. 1.—Example of the simulated light curves according to our proposed observational strategy for the next generation microlensing survey. The parameters of the light curve are chosen to be $t_e = 100$ days, $t_0 = 365$ days, $u_0 = 0.3$, $b = 0.88$, and $R = 0.5$. The background star is chosen to have an apparent magnitude of 22. The dashed and solid lines show the result of least-squares fit of the Schwarzschild and NUT theoretical light curves to the simulated data, respectively. The reconstructed NUT parameter derived from the fitting is $R_{\rm rec} = 0.501668$, with 1 σ uncertainty of 0.001946; $\chi^2/N_{\rm dof}$ for this light curve from the NUT and the Schwarzschild fittings are 0.26 and 30.88.

3.1. *Simulation of Light Curves*

The aim of this section is to simulate the microlensing light curves according to the observational strategy described above. We use the theoretical light curves to fit the simulated ones and evaluate the magnetic mass parameter of the NUT metric. The final result of this procedure is the observational magnetic mass detection efficiency, which can be applied to different galactic models. To start simulating the light curves, we use a uniform random function to generate the lens parameters.

The standard microlensing light curve in the Schwarzschild metric depends on four parameters: the base flux F_b, minimum impact parameter u_0, duration of the event t_e, and moment of minimum impact parameter or maximum magnification t_0. Taking into account the magnetic mass needs an extra parameter, R. The relevant parameters in simulating the light curves are chosen in the intervals $u_0 \in [0,\ 1]$, $t_0 \in [0,\ 2]$ yr, $t_E \in [5,\ 365]$ days, and $R \in [0,\ 0.5]$.

The base fluxes F_b of the background stars in the direction of the LMC are chosen according to the magnitude distribution in the EROS catalogs (Lasserre 2000). Since it has been shown that the contribution of the blending effect is important

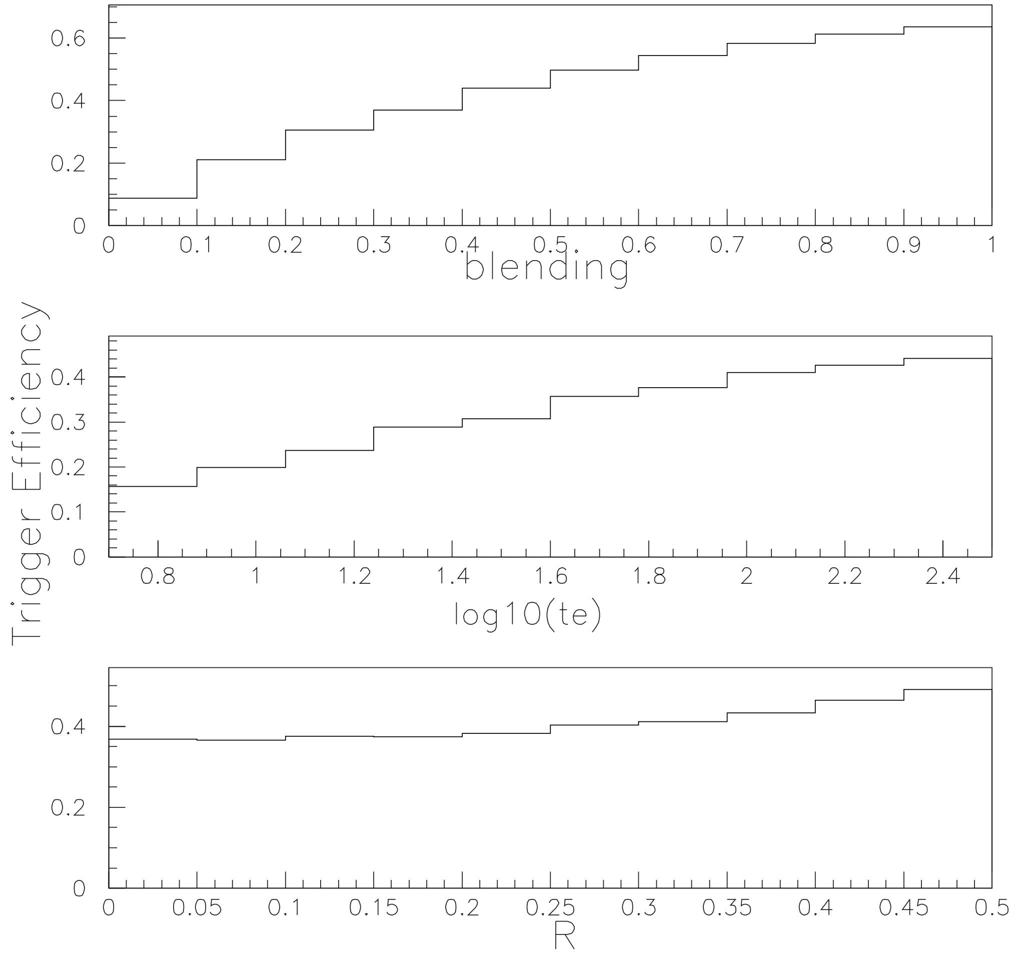

FIG. 2.—Trigger efficiency in terms of the blending parameter (*top*), duration of events (*middle*), and R (*bottom*). The efficiency of the alert system depends on the blending parameter. This means that the larger blending factors produce a lower maximum magnification. In addition, for the long-duration events there is a greater chance of being alerted by the primary telescope. For events with larger R, the peak of maximum magnification is elevated, resulting in a greater probability that those events will be alerted.

in this study, we use the blending distribution that has been obtained from the observed LMC microlensing events in order to use them in generating the light curves (Alcock et al. 2000). The light curves are simulated using the sampling rate of EROS, which is about one observation per six nights on average and is variable during the seasons. The average relative photometric precision $\Delta F/F$ for a given flux F (in ADU) is taken from the EROS phenomenological parametrization, which has been found for a standard quality image (Derue 1999).

In simulating the light curves, every photometric measurement is randomly shifted according to a Gaussian distribution that reflects the photometric uncertainties. Since the photometric uncertainty depends on the apparent magnitude of the background stars, the error bars of the light curves decrease by increasing the brightness of background source during the lensing (see Fig. 1).

3.2. *Simulation of a Simple Alert System*

The next step is to simulate an alert system to trigger observation of the ongoing events and the follow-up observation by the secondary telescope. According to one of the EROS alert algorithms, the events are announced as soon as their light curves exhibit four consecutive flux measurements above 4 σ from the base line (Mansoux 1997). It is clear that only the

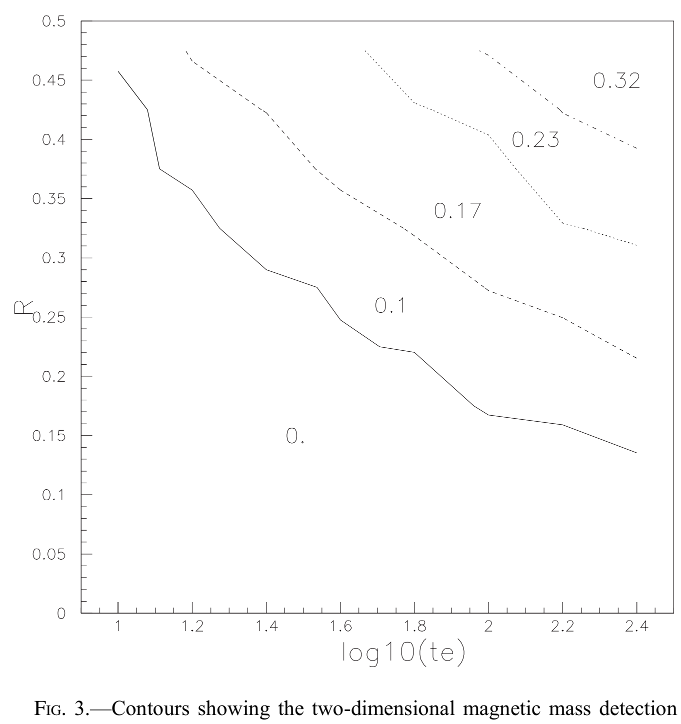

FIG. 3.—Contours showing the two-dimensional magnetic mass detection efficiency in terms of duration of events and R. The numbers between the contours show the level of detection efficiency.

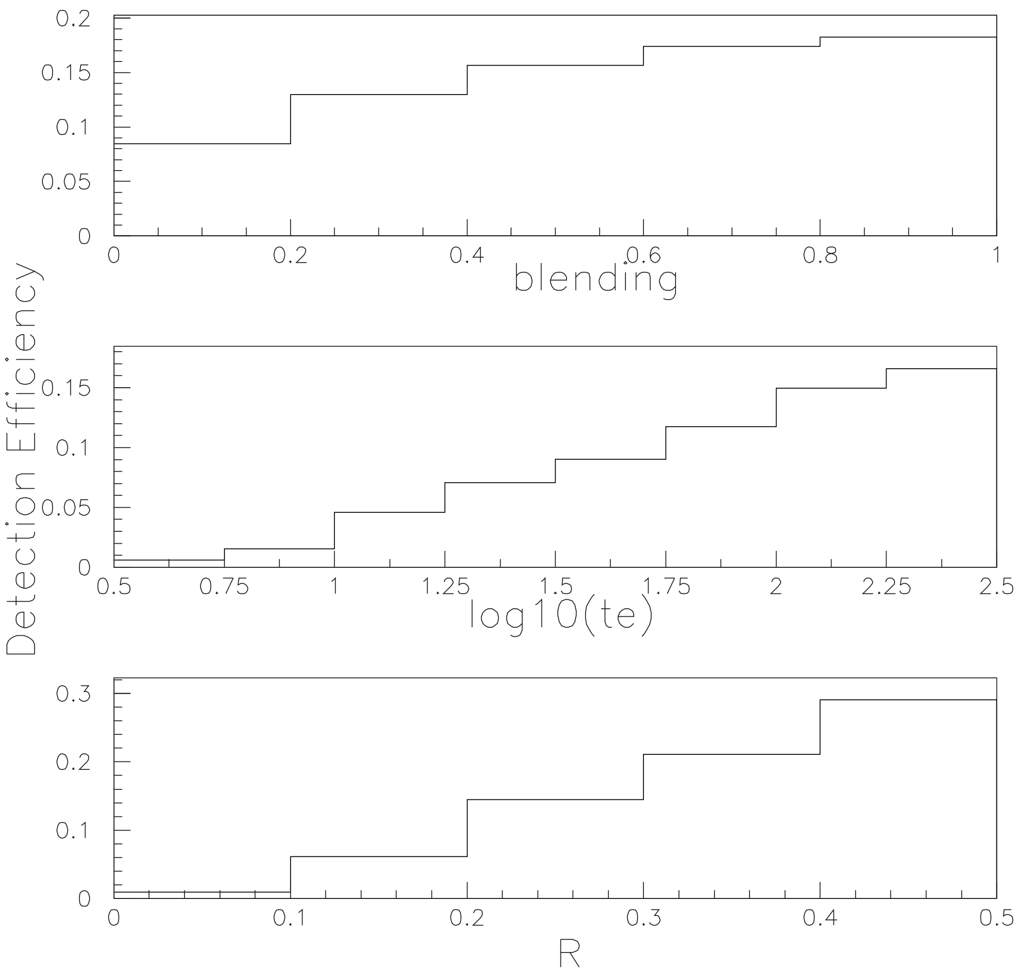

FIG. 4.—Magnetic mass detection efficiency in terms of blending parameter (*top*), duration of events (*middle*), and R (*bottom*). According to the top panel, the magnetic mass effect can be dominated by the blending. The detection efficiency also has a direct dependence on the duration of events and R. A rough estimate of the minimum R that can be detected is about $R = 0.1$.

most significant microlensing events are selected by this algorithm. We have in fact considered several trigger thresholds, from a loose criterion (three consecutive measurements above 3 σ from the base line) to the strict criterion that was finally used. Even using this strict criterion, on average one false alarm due to variable stars or instrumental artifacts is expected per true microlensing alert (J.-F. Glicenstein 2002, private communication). This false-alarm rate will induce some lost follow-up time, but of very limited duration, as it is usually possible to quickly identify and discard a non-microlensing event. Figure 1 shows an example of a microlensing light curve that has been simulated using the specifications of the primary and secondary follow-up telescopes.

The efficiency of the alert system depends on the parameters of the lenses. In order to obtain the trigger efficiency in terms of physical parameters such as the duration of events and R, we integrate over irrelevant parameters such as the minimum impact parameter and the time of maximum magnification. Equation (2) shows that the NUT parameter increases the maximum magnification, or in other words decreases the effective minimum impact factor. The result is a higher trigger rate for microlensing events that have larger R. This effect is shown in Figure 2. It shows that the trigger efficiency is increased by the longer duration of microlensing events, which reflects a greater probability of observing long-duration events than short ones.

4. FOLLOW-UP TELESCOPE AND FITTING PROCESS TO THE LIGHT CURVES

We use a Monte Carlo simulation to generate a large number of microlensing events. At the first step the lens parameters are chosen and the light curve is generated according to the primary telescope specification. Using the trigger system, in the case that an event is alerted, the secondary telescope starts its measurements of the ongoing microlensing event with high sampling rate and photometry precision.

The second telescope is supposed to be a partially dedicated telescope, which follows the measurements of alerted events. The telescope is assumed to have about 1% precision in photometry and to sample events through all clear nights. According to the meteorological statistics of La Silla observatory, about 70% of nights per year are clear. A 1 m telescope could achieve this precision with a long exposure of about 30 minutes.

After simulating a large number of events by this strategy, we use the NUT and Schwarzschild theoretical microlensing light curves to fit the simulated ones. The least-squares method is used to fit the theoretical light curves on the data. An example of the fitting routine is shown in Figure 1. When fitting data with the NUT curve with $R < 0.1$, we encounter the degeneracy problem, which means that for R close to zero we may obtain from the fitting a nonzero reconstructed value for R. To distinguish between the microlensing light curves affected by NUT charge and the standard ones, we use the criterion that $\Delta\chi^2 > 2$, where

$$\Delta\chi^2 = \frac{\chi^2_{\rm Sch} - \chi^2_{\rm NUT}}{\chi^2_{\rm NUT}/N_{\rm dof}} \frac{1}{\sqrt{2N_{\rm dof}}}, \qquad (5)$$

where indices of the χ^2 correspond to the type of the metric, and $N_{\rm dof}$ is the number of degree of freedom in the NUT fitting. As a complementary criterion, we require the signal-to-noise ratio of R to be more than 2. We obtain the magnetic mass detection efficiency of MACHOs by dividing the reconstructed parameters of those events that meet these two criteria by the generated events. Figure 3 shows the two-dimensional efficiency of magnetic mass detection in terms of R and the duration of events.

The detection efficiency of magnetic mass has a direct correlation with R as well as with the duration of the events. It is more practical to obtain efficiencies in terms of duration of events and R, which are shown in Figure 4. It should be mentioned that the blending effect decreases the detection efficiency of magnetic mass, as also shown in Figure 4.

5. CONCLUSION

In this work we propose a new strategy for microlensing observation that not only can be used for searching for MACHOs in the Galactic halo by observing LMC stars, but also can be a useful tool to explore exotic spacetimes around compact objects, such as the NUT metric. As a result of our Monte Carlo simulation, we obtained the detection efficiency for magnetic mass. The minimum value for R that can be observed by this method is about 0.1. In order to evaluate the amount of detectable magnetic mass l, we use the relation between the magnetic mass and R (Rahvar & Nouri-Zonoz 2003),

$$R = c\sqrt{\frac{l}{2GM}}. \qquad (6)$$

EROS and MACHO experiments results propose that the mean value of the mass of MACHOs is about 0.5 $M_\odot$ (Alcock et al. 2000; Lasserre et al. 2000). It is worth mentioning that this result is obtained in the standard halo model, where the mean mass of MACHOs depends on the model that is used for the Milky Way. Assuming standard model for the Milky Way halo, according to equation (6) the minimum observable magnetic mass l is evaluated to be about 14 m. The absence of a magnetic mass signal in the microlensing light curves can also set an upper limit of $l < 14$ m in the MACHOs of the Milky Way.

The authors thank M. Nouri-Zonoz, H. Hakimi Pajouh, and S. Arbabi Bidgoli for their useful comments.

REFERENCES

Adams, F., & Laughlin, G. 1996, ApJ, 468, 586
Alcock, C., et al. 2000, ApJ, 542, 281
Canal, R., Isern, J., & Ruiz-Lapuente, P. 1997, ApJ, 488, L35
Chabrier, G., Segretain, L., & Mera D. 1996, ApJ, 468, L21
Demircan, O., & Kahraman, G. 1990, Ap&SS, 181, 313
Derue, F. 1999, Ph.D. thesis, Univ. Paris (CNRS/IN2P3, LAL Rept. 99-14)
Evans, N. W. 1994, MNRAS, 267, 333
Gates, I. E., & Gyuk, G. 2001, ApJ, 547, 786
Green, A. M., & Jedamzik, K. 2002, A&A, 395, 31
Gyuk, G., Dalal, N., & Griest, K., 2000, ApJ, 535, 90
Lasserre, T. 2000, Ph.D. thesis, Univ. Paris (CNRS/IN2P3, LAL Rept. 97-19)
Lasserre, T., et al. 2000, A&A, 355, L39
Mansoux, B., 1997, Ph.D. thesis, Univ. Paris (CNRS/IN2P3, LAL Rept. 97–19)
Newman, E. T., Tamburino, L., & Unti, T. 1963, J. Math. Phys., 4, 915
Nouri-Zonoz, M., Lynden-Bell, D. 1997, MNRAS, 292, 714
Paczyński, B. 1986, ApJ, 304, 1
Palanque-Delabrouille, N., et al. 1998, A&A, 332, 1
Popowski, P., et al. 2000, BAAS, 32, 1391
Rahvar, S. 2004, MNRAS, 347, 213
Rahvar, S., Moniez, M., Ansari, R., & Perdereau, O. 2003, A&A, 412, 81
Rahvar, S., & Nouri-Zonoz, M. 2003, MNRAS, 338, 926
Wozniak, P., & Paczynski, B. 1997, ApJ, 487, 55